Available online at www.sciencedirect.com

SCIENCE DIRECT

Biochimica et Biophysica Acta 1758 (2006) 702–712

BIOCHIMICA ET BIOPHYSICA ACTA BBA

http://www.elsevier.com/locate/bba

Reciprocal inhibition of Cd^{2+} and Ca^{2+} uptake in human intestinal crypt cells for voltage-independent Zn-activated pathways

Pierre-Michel Bergeron, Catherine Jumarie *

Département des Sciences Biologiques, Centre TOXEN, Université du Québec à Montréal, C.P. 8888, Succ. Centre-ville, Montréal (Québec), Canada H3C 3P8

Received 3 November 2005; received in revised form 19 April 2006; accepted 26 April 2006
Available online 19 May 2006

Abstract

Cadmium–Ca–Zn interactions for uptake have been studied in human intestinal crypt cells HIEC. Our results failed to demonstrate any significant cross-inhibition between Cd and Ca uptake under single metal exposure conditions. However, they revealed a strong reciprocal inhibition for a Zn-stimulated mechanism of transport. Optimal stimulation was observed under exposure conditions that favor an inward-directed Zn gradient, suggesting activation by extracellular rather than intracellular Zn. The effect of Zn on the uptake of Ca was concentration-dependent, and zinc-induced stimulation of Cd uptake resulted in a 3- and 5.8-fold increase in the K_m and V_{max} values, respectively. Neither basal nor Zn-stimulated Ca uptakes were sensitive to membrane depolarization. However, the stimulated component of uptake was inhibited by the trivalent cations Gd^{3+}, and La^{3+} and to a lesser extent by Mg^{2+} and Ba^{2+}. RT-PCR analysis as well as uptake measurement performed with extracellular ATP and/or suramin do not support the involvement of purinergic P2X receptor channels. Uptake and fluorescence data led to the conclusion that Zn is unlikely to trigger Ca influx in response to Ca release from thapsigargin-sensitive intracellular pools. Our data show that Zn may potentiate Cd accumulation in intestinal crypt cells through mechanism that still needs to be clarified.

Keywords: Cadmium; Calcium; Zinc; Intestinal crypt cell; P2XR; SOCs; CRAC; Zn-sensing receptor

1. Introduction

Cadmium (Cd) is a non-essential heavy metal that is massively emitted into the environment as a result of human activities, including industrial uses [1]. Cadmium has a broad range of adverse effects, and its long biological half-life – about 30 years in humans – makes it an insidiously toxic metal [2]. Therefore, absorption is the determinant step in Cd accumulation in the organism. Although pulmonary absorption predominates in occupationally exposed workers and heavy smokers, intestinal intake represents the main route for Cd absorption for the general population.

Intestinal absorption of Cd is likely to involve mainly transcellular pathways to cross the intestinal epithelium [3]. In vivo and in vitro studies have shown that Cd may inhibit the intestinal transport of essential elements such as Ca [4–6] and Zn [7–11]. Alhtough Cd uptake through Ca transport processes at the apical membrane of the enterocyte remain to be clarified, it is generally believed that Cd accumulation in intestinal cells may, at least in part, occur through transport systems responsible for Ca or Zn uptake. More recently, we and others have shown that the symport H^+-Fe^{2+}NRAMP2 is involved in the apical uptake of the free cation Cd^{2+} in human enterocytic-like Caco-2 cells [12–14]. We have also provided evidence for the uptake of inorganic as well as organic Cd complexes in the same cells [15].

Despite their expected minor role in intestinal absorption processes, proliferative intestinal crypt cells, which undergo enterocytic differentiation during their migration along the crypt–villus axis, may also be exposed to Cd following oral intake. Indeed, in vivo studies have demonstrated the presence of significant levels of Cd accumulation in the crypt area of the intestinal epithelium [16–18]. Because of the critical role that proliferative crypt cells play in intestinal epithelium renewal, the study of Cd uptake and toxicity in these cells is of primary interest. Recently, we characterized Cd uptake in HIEC cells [19]. This non-tumorous, non-transformed human crypt cell line has been established by thermolysin treatment of 17- to 19-week

* Corresponding author. Fax: +1 514 987 4647.
E-mail address: jumarie.catherine@uqam.ca (C. Jumarie).

0005-2736/$ - see front matter © 2006 Elsevier B.V. All rights reserved.
doi:10.1016/j.bbamem.2006.04.019

fetal ileums and express various intestinal cell markers including the intestinal-specific keratins 8, 18 and 21 [20]. They also express the MIM-1/39-specific antigen for intestinal crypt cells but lack the brush border membrane enzymes sucrase-isomaltase and maltase-glucoamylase specific to the mature enterocyte. These cells have been used in a number of studies focusing on cell cycle progression and MAPK signalling [21,22], integrin expression [23,24], intestinal cell turn-over and enterocytic differentiation [25,26], as well as apoptosis [27]. We have shown that Cd is rapidly and significantly accumulated in these cells through specific (saturable) transport mechanism(s) [19]. We also provided evidence of a preferential uptake of the free cation Cd^{2+} over $CdCl_n^{2-n}$ chlorocomplex species. However, and contrary to what we have observed for the highly differentiated TC7 clone of the parent cell line Caco-2, Cd^{2+} uptake in HIEC cells does not involve NRAMP2 [19]. Although in a small proportion, Ca alone or in combination with Zn inhibited the uptake of Cd in these cells, and part of the Cd uptake was also sensitive to La. [19]. We pursued our studies on the mechanisms involved in Cd uptake in HIEC cells, focusing on Cd interactions with Ca and Zn. Our results reveal that Zn may stimulate either Cd or Ca uptake, with this stimulatory effect being eliminated by the presence of Ca and Cd, respectively. Two possible mechanisms have been investigated: Zn action through P2 receptors or through Zn-sensitive receptor. P2X receptors (P2XRs) are extracellular ATP-gated non-selective cation channels that allow influx of extracellular Ca [28], and Zn has been shown to potentiate $P2X_4$ purinergic receptor channel-mediated Ca^{2+} influx [29–32]. On the other hand, Zn-sensing receptor (ZnR) has also been shown to trigger the release of thapsigargin-sensitive Ca pool in a PLC-dependent manner [33]. However, our results do not support the involvement of voltage-gated Ca channels or purinergic P2X channels or store-operated channels (SOCs) in Zn-induced stimulation of metal uptake.

2. Materials and methods

2.1. Cell culture

HIEC cells were kindly supplied by Dr. Jean-François Beaulieu (Université de Sherbrooke, Sherbrooke, QC, Canada) [20]. Stock cultures were seeded in 75-cm^2 flasks (Sarstedt) at a density of 2×10^6 cells/flask and maintained in a 37 °C, 5% CO_2 humidified atmosphere. Cultures were grown in Dulbecco's modified Eagle essential minimum medium (DMEM) containing 25 mM glucose (GibcoBRL, Grand Island, New York, USA) and supplemented with 19 mM $NaHCO_3$, 20 mM HEPES, 5 μg/l epidermal growth factor (BD Biosciences, Mississauga, ON, Canada), 200 U/l insulin, 10 ml/l Glutamax™ (GibcoBRL), penicillin–streptomycin (50,000 U/l–50 mg/l), and 5% heat-inactivated fetal bovine serum (FBS) (Medicorp Inc., Montreal, QC, Canada). The medium was changed every other day, and confluency was reached in 7–8 days. For uptake experiments, cells were passaged with 0.05% trypsin–0.53 mM EDTA (GibcoBRL) for 5–10 min, then seeded at a density of 0.12×10^6 cells/dish in 35-mm-diameter culture dishes, and cultured as previously described [19]. HIEC cells were used between passages 19 and 28.

The highly differentiated TC7 clone (passages 65) of the enterocytic-like cells Caco-2 (obtained from Dr. A. Zweibaum, INSERM U178, Villejuif, France) [34] was maintained in DMEM (25 mM glucose), supplemented with 0.1 mM non-essential amino acids, penicillin–streptomycin (50,000 U/l–50 mg/l) and 15% inactivated FBS. As for the HIEC cells, stock cultures were grown in 75-cm^2 flasks. For RT-PCR analysis, both HIEC and TC7 cells were seeded in 100-mm-diameter culture dishes at a density of 12×10^3 cells/cm^2 and were maintained at 37 °C in a 5% CO_2 humidified air atmosphere.

The human alveolar type II cells A549 (passage 85), obtained from the American Type Culture Collection, were maintained in Ham's F12 medium (50,000 U/l penicillin, 50 mg/l streptomycin) supplemented with 10% FBS and 1 mM glutamine. Cells were routinely grown in 75-cm^2 culture flasks at 37 °C in a 5% CO_2–95% humidified air atmosphere and were seeded in 100-mm-diameter Petri dishes at a same density as for TC7 cells.

2.2. Measurements of Cd and Ca uptake

Uptake measurements were performed at room temperature under inorganic conditions using a serum-free nitrate incubation (transport) medium containing (in mM) 10 HEPES, 4 D-glucose, 137 $NaNO_3$, 5.9 KNO_3, 2.5 $Ca(NO_3)_2$ and 1.2 $MgSO_4$, buffered to pH 7.4 with NaOH. When appropriate, Ca and Mg were both removed and replaced by Na to maintain osmolarity. The uptake media were always prepared in advance and allowed to reach equilibrium overnight at room temperature. The chemical species of Cd (or Ca) in the incubation media, namely metal speciation, were calculated using the MINEQL$^+$ chemical equilibrium program [35] and the NIST stability constant database [36]. In the present study, a nitrate uptake medium, rather than a traditional chloride medium, was used to optimize the level of the free cation Cd^{2+} over chlorocomplex formation [12,15]. Indeed, the inorganic ligand Cl^- has a very high affinity for the Cd^{2+} aquo ion (log K_c $CdCl^+=1.98$, where K_c, corrected for zero ionic strength, is the conditional formation constant for Cd complexation), and most of the total dissolved metal (84%) would be present in the chloride uptake medium as $CdCl_n^{2-n}$ chlorocomplexes. Because NO_3^- does not bind Cd^{2+} as much as does Cl^- (log K_c $CdNO_3^+=0.50$), substituting Cl^- for NO_3^- in the transport medium results in a 5.7-fold increase in the relative level of Cd^{2+} (14% to 80% of the total dissolved metal). Contrary to Cd, Ca complexation by chloride is weak (log K_c $CaCl^+=0.64$ compared to log K_c $CaNO_3^+=0.50$); therefore, Ca speciation does not significantly change, regardless of the exposure medium used, and most of the dissolved Ca is present as Ca^{2+} (83% and 97% in the chloride and nitrate medium, respectively). It has been verified that the anionic ligand NO_3^- does not modify membrane permeability, and the Cd uptake properties measured in the nitrate medium were similar to the perchlorate or gluconate uptake conditions [19].

Ten-day-old cell cultures with dense confluency (passages 19 to 28) were rinsed four times with a chloride medium (transport medium where NO_3^- was changed for Cl^-) in order to remove the culture medium, which contains various organic ligands that lower considerably the level of the total dissolved metal present as the free aquo ion and that do not allow metal speciation to be controlled. In some cases, cells were incubated for 15 min in a Na-free (excess of K) chloride medium prior to the uptake measurements. Also, a 15-min pretreatment with Ca- and Mg-free chloride medium containing various levels of Zn was used in some other experiments. Cell monolayers were then exposed to 0.3 μM ^{109}Cd-labeled $CdCl_2$ (specific activity ranging from 2.6 to 3.8 mCi/mg) (Perkin Elmer Life Science, Woodbridge, ON, Canada) in either Ca-, Mg-free (control) or Ca-, Mg-containing nitrate medium. Ca uptake measurements were performed using 2.5 μCi/ml ^{45}Ca-labeled $CaCl_2$ (Perkin Elmer Life Science) in Mg-free nitrate medium containing 0.5 mM total Ca (specific activity was then set at 5 μCi/μmol). In the present study, Ca uptake data are expressed relative to the total Ca (2.5 μCi/ml ^{45}Ca+0.5 mM Ca), whereas uptake data for Cd are relative to the tracer (0.3 μM ^{109}Cd) exclusively. In some experiments, uptake measurements were conducted in the presence of different concentrations of Zn or 1 mM magnesium (Mg), barium (Ba), gadolinium (Gd) or lanthanum (La). Nifedipine or verapamil (10 μM), two well-known voltage-gated Ca channel blockers, were also tested for their putative inhibitory effect. The involvement of the purinergic P2X receptor channels in Ca and Cd uptake has been tested using extracellular ATP (50 μM) or suramin (30 μM), a P2X antagonist [37]. The possible involvement of store-operated channels (SOCs) has been tested using 30 μM 1-[β-[3-(4-methoxyphenyl)propoxy]-4-methoxyphenethy]-1H-imidazole hydrochloride (SKF-96365) [38], whereas 2 μM U73122 was used to inhibit any phospholipase C (PLC)-dependent channel activation [33]. The presence of SOCs in HIEC cells has been studied with cell pretreatment with 0.5 μM thapsigargin, an inhibitor of the sarco/endoplasmic reticulum (ER) Ca^{2+}-ATPase (SERCA), for 5 min prior Ca addition. For nifedipine, verapamil, thapsigargin and U73122, stock solutions were prepared in DMSO (with appropriate control

exposure conditions) and were protected from light. ATP solutions were prepared daily.

After the desired exposure times, the transport medium was removed, and the dishes were rapidly rinsed four times with ice-cold Ca-, Mg-free nitrate medium containing 2 mM EDTA, used to minimize metal adsorption at the external surface of the cell membrane. Cells were lysed in 500 μl NaOH 1N, and 300 μl was used for radioactivity determination. ^{109}Cd contents were assayed with a Cobra II gamma counter (Canberra Packard, Canada), whereas ^{45}Ca contents were assayed with a Wallac 1409 DSA liquid scintillation counter (Wallac Oy, Turku, Finland). 50 μl of the remaining cell suspension was used for protein determination according to Bradford [39] with a Tecan SpectraFluor Plus spectrophotometer (Esbe Scientific Industries Inc., Canada) and bovine serum albumin as the calibration standard.

2.3. Florescence measurements of intracellular Ca

Five-day-old HIEC cells were rinsed four times with the chloride medium prior incubation with 2 μM Fluo-3/AM and 10% Pluronic F127 (Molecular Probes Corp. Eugene, OR) for 45 min at 37 °C in the dark. The cells were then washed with the chloride medium and incubated for another 45 min at room temperature in the dark to ensure dye deesterification. Following transfer to a Ca-, Mg-free nitrate medium, additions were made in an open chamber configuration at room temperature. The cells were examined with a laser scanning MRC 1024 confocal system (Bio-Rad Laboratories Ltd., Mississauga, ON) with a TE-300 inverted microscope (Nikon Canada Inc., Mississauga, ON) and an apochromatic 40× N.A. 1,0 objective lens. Fluo-3 fluorescence was measured using an excitation wavelength of 488 nm (argon laser) and an emission filter at 515 nm. Ca release from ER was activated by the addition of 5 μM thapsigargin. Thereafter, SOCs activation was clearly observed following addition of 0.5–1.0 mM Ca. Inhibition of SOCs was accomplished by addition of SKF-96365. The effect of SKF-96365 on Zn-induced increases in intracellular Ca was also tested. Data were analyzed with Laser Sharp 2.1T, Time Course 1.0 software and are expressed as fluorescence levels relative to control (F/F_0 ratio).

2.4. Isolation of total RNA

Glassware and water used for solutions and RNA isolation were made RNase-free by treating them with 0.1% diethylpyrocarbonate (DEPC) and autoclaving. For each experimental condition, cells from five 100-mm-diameter Petri dishes were pooled to obtain sufficient material. Total RNA was extracted from the HIEC, the TC7 and the A549 cells by means of TRIZOL® reagent (Invitrogen Life Technologies, Burlington, ON, Canada), according to the supplier's instructions. Poly A$^+$RNA was purified from total RNA using the Oligotex® mRNA Mini Kit (Qiagen, Mississauga, ON, Canada). The mRNA pellets were dried and then dissolved in 30–50 μl DEPC-treated water. The purity and concentration of the samples were assessed using a Beckman DU® 650 spectrophotometer (Beckman Coulter Canada) at 260 and 280 nm: 260 to 280 nm absorbance ratios higher than 1.7 were considered as acceptable, whereas 1 U of A_{260} was equivalent to 40 μg RNA. In addition, RNA integrity was verified by the presence of ribosomal RNA (ethidium bromide staining of the 18 S and 28 S bands) following agarose gel electrophoresis.

2.5. Reverse transcriptase (RT) and polymerase chain reaction (PCR) of P2X4 cDNA

The levels of $P2X_4$ mRNA were estimated by semi-quantitative RT-PCR. Reverse transcriptase was performed with 2 μg mRNA using the Omniscript® RT Kit (Qiagen) according to the supplier's instructions, and PCR was conducted with 1 μl cDNA using the Taq PCR Core Kit (Qiagen). 40 and 30 cycles consisting of: denaturation at 94 °C for 1 min, annealing at 58 °C for 30 s, and extension at 72 °C for 1 min were carried out for $P2X_4$ and GAPDH cDNA amplification, respectively. The sense and antisense primer sequences for $P2X_4$ were 5′-GGCCTTCCTGTTCGAGTACG and 5′-TGGGAAGGATATTCC-TCTTGC, respectively (GenBank U83993, bases 336–931). The sense and antisense primer sequences for GAPDH used as an internal control were 5′-GAGTCAACGGATTTGGTCGTATTG and 5′-GCTGTAGCCAAATT-CGTTGTC, respectively (GenBank AF261085, base 123–1066). The primers amplify a fragment of 596 and 944 for $P2X_4$ and GAPDH, respectively. The PCR products were resolved on 2.0% (w/v) agarose gels containing 0.05 μg/ml ethidium bromide and visualized under UV trans-illumination using an LKB 2011 Macrovue Fluorescence system controlled by AlphaImager™ 2200 software (Alpha Innotech Corporation, San Leandro, California, USA).

2.6. Statistical and data analyses

All experiments were performed on 3 to 5 independent cell preparations, and in each case, on 3 to 5 culture dishes. Uptake time courses of Cd were analyzed according to the first-order rate Eq. (1),

$$U = U_{\max}(1 - e^{-kt}) + U_0, \tag{1}$$

where U_0 and $U_{\max}$ are the zero-time and equilibrium uptake values, respectively, the latter reached with the time constant k.

Estimation of the first-order rate constant allows the $t_{½}$ values to be determined, which represent the times at which metal uptake is half-completed, using Eq. (2),

$$t_{1/2} = \frac{\ln 2}{k}. \tag{2}$$

The kinetic parameters of ^{109}Cd uptake were determined by analyses of the one-time point measurements at 3-min (v_3) according to the modified Michaelis-Menten Eq. (4),

$$v_3 = \frac{V_{\max}[^{109}Cd]}{K_m + [^{109}\mathrm{Cd}] + [\mathrm{Cd}]} + k_D[^{109}\mathrm{Cd}], \tag{3}$$

where $V_{\max}$ and K_m have their usual meaning, [^{109}Cd] was set at 0.3 μM, whereas [Cd] increased from 0 to 100 μM, and k_D represents the non-specific contributions to the 3-min uptake data.

The concentration-dependent stimulation of the initial 3-min uptake ($U_{3[Zn]}$) of Ca by Zn was analyzed assuming a simple (non-cooperative) mechanism using Eq. (4),

$$U_{3[Zn]} = U_{3(0)} + \frac{U_{3(\max)}[\mathrm{Zn}]}{\mathrm{EC}_{50} + [\mathrm{Zn}]}, \tag{4}$$

where $U_{3(0)}$ and $U_{3(max)}$ stand for the 3-min uptake values measured at 0 and maximal Zn concentration, respectively, and EC_{50} is the Zn concentration ([Zn]) for which half-maximal stimulation is observed at [Ca]=0.5 mM.

Nonlinear regression analyses were performed with Prism 3 software (GraphPad Software, San Diego, California, USA). The errors associated with the kinetic parameter values given in the text represent the standard error of regression (SER). Statistical analyses of the 3-min measurements were performed with Turkey-Kramer multiple comparison tests, using InStat software (GraphPad Software). Differences among groups were tested using one-way analysis of variance (ANOVA), followed by a Dunnett's test to compare treated groups with controls. Statistical significance was assessed at the $P \leq 0.05$ level.

3. Results

3.1. Stimulatory effect of Zn on Cd and Ca uptake

Metal interactions for uptake were first investigated by studying the reciprocal inhibition between Ca and Cd accumulation in the absence or presence of Zn. As shown in Fig. 1A, the addition of 2.5 mM Ca to the nitrate exposure medium resulted in a non-significant 13% decrease in the 3-min uptake of 0.3 μM Cd (gray column). In contrast, 100 μM Zn led to an unexpected 1.8-fold increase in Cd accumulation (crossed vs. white columns). This stimulation was also observed in the chloride medium as well as at pH 5.5 (data not shown). However, Zn-

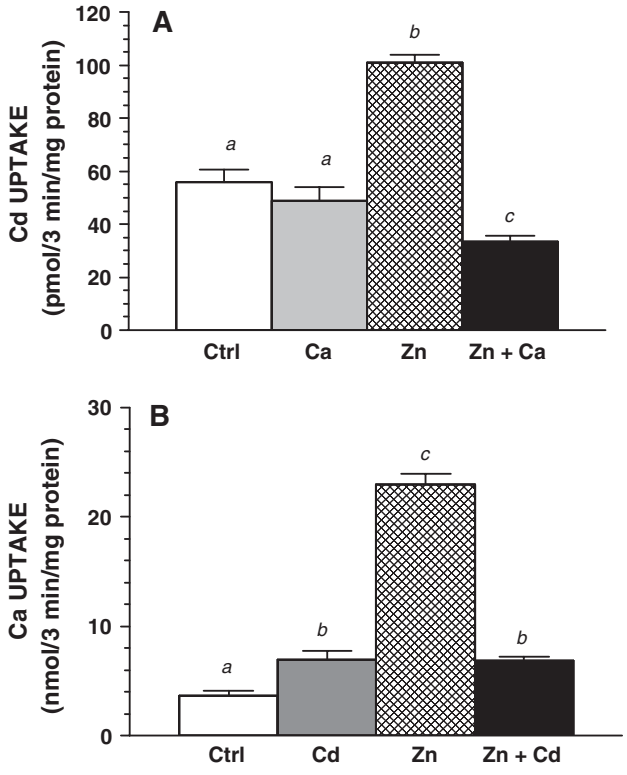

Fig. 1. Short-term (3 min) uptake of 0.3 μM Cd (A) or 0.5 mM Ca (B) in 10-day-old confluent HIEC cell monolayers measured in the absence (Ctrl) or presence of 2.5 mM Ca (A), 100 μM Cd (B) or 100 μM Zn (A and B), alone or in combination with Ca or Cd. Values shown are means±S.D. evaluated on 4 determinations of the same subculture. Columns labeled with different letters are significantly different ($P \leq 0.05$).

induced stimulation of Cd uptake was optimal under nitrate conditions at pH 7.4. It is noteworthy that Ca completely eliminated the stimulatory effect of Zn. Note also that Zn favors Ca-induced inhibition of Cd uptake since significant 40% lower accumulation values were obtained in the presence of co-incubation with Zn and Ca compared to the control value (compare black vs. white columns).

Conversely, the presence of 100 μM Cd did not inhibit Ca uptake but led instead to a significant 1.9-fold increase in accumulation levels (Fig. 1B). As for Cd, Zn stimulated Ca accumulation, but much more than to Cd (6.2-fold). This stimulatory effect was also eliminated by the presence of Cd: similar uptake levels were measured for Ca in the presence of Cd whether or not Zn was added to the incubation medium. Note that Zn failed to stimulate either Ca or Cd uptake in differentiated 21-day-old TC7 cells as well as in 14-day-old A549 cells (Fig. 2).

The concentration–response relationship of Zn-induced stimulation of Ca accumulation measured in a nitrate medium at pH 7.4 was characterized (Fig. 3). The initial 3-min uptake data were analyzed using Eq. (4). An EC_{50} (Zn concentration leading to half-maximal stimulation of Ca uptake) value of 18.3±4.0 μM was estimated for 0.5 mM Ca, while $U_{3(max)}$ (the 3-min uptake measured under maximal stimulatory conditions) was 19.8±1.2 nmol/3 min/mg protein, which is in accordance with previous observation (Fig. 1B).

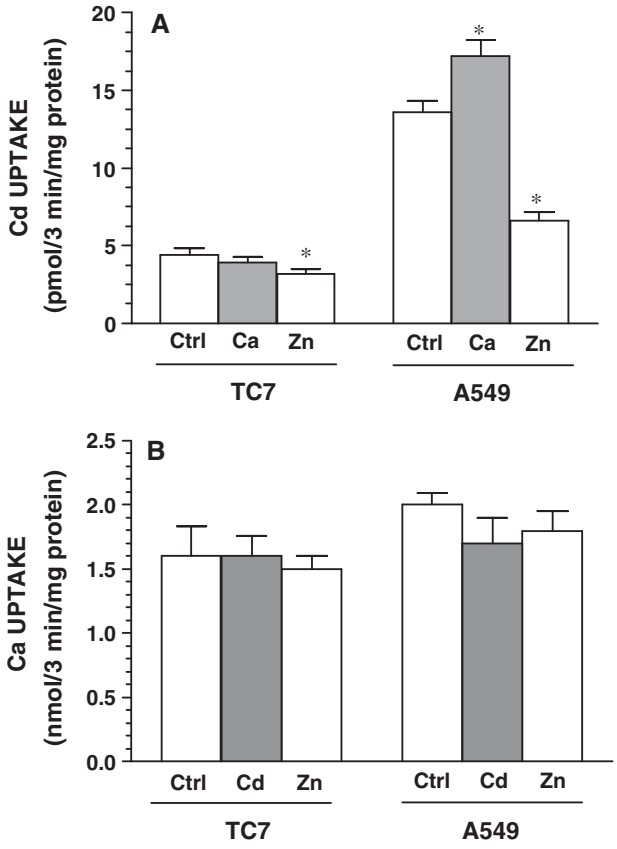

Fig. 2. Short-term (3 min) uptake of 0.3 μM Cd (A) or 0.5 mM Ca (B) in 21-day-old confluent TC7 and 14-day-old A549 cell monolayers, respectively. Uptake was measured in the absence (Ctrl) or presence of 2.5 mM Ca (A), 100 μM Cd (B) or 100 μM Zn (A and B). Values shown are means±S.D. evaluated on 5 determinations of the same subculture. *Significant differences ($P \leq 0.05$) compared with the respective control value for each cell line.

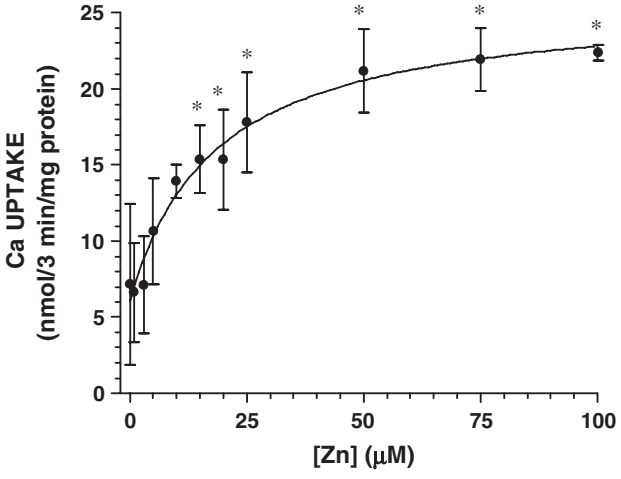

Fig. 3. Short-term (3 min) accumulation of 0.5 mM Ca in 10-day-old HIEC cells as a function of increasing concentrations of unlabeled Zn. Points shown are means±S.D. evaluated on 3 different cell preparations. The line shown is the best-fit curve for the data points as obtained according to Eq. (4) with the following parameter values: $v_{3(0)}$=6.1±0.7 nmol/3 min/mg protein, $v_{3(max)}$=19.8±1.2 nmol/3 min/mg protein, and EC_{50}=18.3±4.0 μM. *Significant differences ($P \leq 0.05$) compared with control values measured in the absence of Zn.

We further characterized the Zn-induced stimulation of Cd and Ca uptake by investigating how much this effect is related to the Zn transmembrane gradient (Fig. 4). Measurements of cellular accumulation were conducted in the absence (open columns) or in the presence of 10 μM (dashed columns), 100 μM (black columns) or 1 mM (crossed columns) Zn in control cells (no pretreatment) or in cells preincubated for 15 min in either 10 or 100 μM Zn. For both Cd (Fig. 4A) and Ca uptake (Fig. 4B), a maximal stimulation was obtained in untreated control cells with 100 μM Zn in the transport medium. The stimulatory effect of Zn decreased with cell pretreatment with 10 μM Zn and was no longer observed in cells preincubated with 100 μM Zn. Interestingly, a bell-shaped concentration–response curve was observed for Zn-induced stimulation in Ca uptake in control cells, whereas a hit-or-miss effect was observed for Cd accumulation.

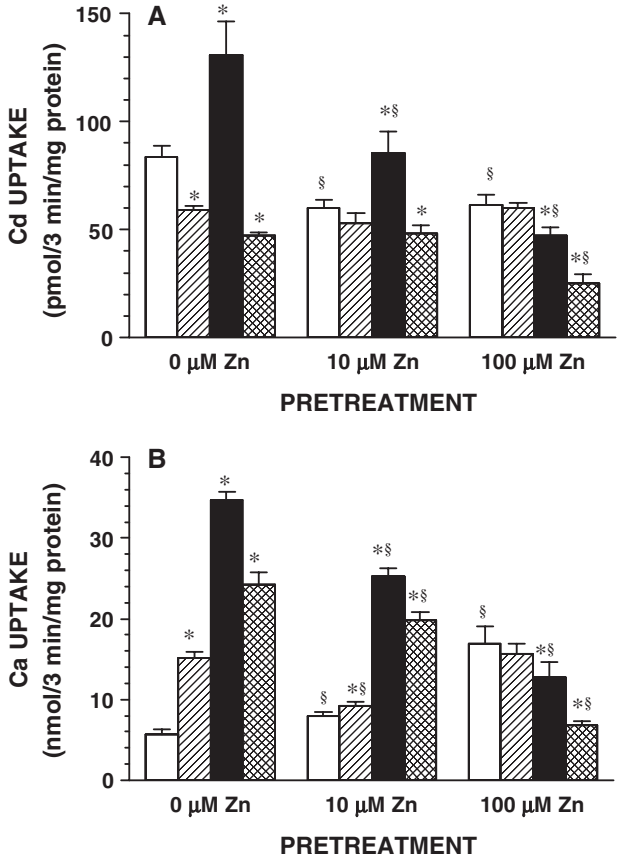

Fig. 4. Short-term (3 min) accumulation of 0.3 μM Cd (A) or 0.5 mM Ca (B) in confluent 10-day-old HIEC cell monolayers in the absence (open columns) or presence of increasing concentrations of Zn: 10 μM (dashed columns), 100 μM (black columns), and 1 mM (crossed columns). Cells were pre-exposed to various concentrations (0, 10 or 100 μM) of Zn for 15 min in the Ca- and Mg-free chloride medium prior to uptake measurements in the nitrate medium. Values shown are means ± S.D. evaluated on 5 determinations of the same subculture. *Significant differences ($P \leq 0.05$) compared with the respective control value for each pretreatment, measured in the absence of Zn in the incubation medium during the uptake measurement. §Significant differences ($P \leq 0.05$) compared with similar uptake conditions on control cells (no Zn pretreatment).

3.2. Influence of Zn on kinetic parameters of Cd uptake

Because oral exposure to toxic metals is likely to involve metal mixtures, the effects of Zn on Cd accumulation were characterized. The uptake time course of 0.3 μM Cd was first studied in the absence (open triangles) and in the presence of 100 μM Zn (filled triangles) (Fig. 5A). Data analyzed according to first-order rate Eq. (1) revealed a 1.3-fold increase in the equilibrium accumulation value reached 2 times faster (parameters U_{max} and $t_{½}$ in Table 1) when Zn was added to the nitrate transport medium.

How Zn may modify the kinetic parameter values of Cd accumulation was also determined by measuring the 3-min uptake of 0.3 μM ^{109}Cd as a function of increasing concentrations of unlabeled Cd in the absence or in the presence of 100 μM Zn (Fig. 5B). In these studies, unlabeled Cd was used as a specific competitive inhibitor of tracer uptake, and data were analyzed according to the modified Michaelis-Menten Eq. (3) with parameter values reported in Table 2. The presence of Zn resulted in a 5.9-fold and 3-fold increase in the V_{max} and K_m values, respectively, while k_D was lowered by 58%.

3.3. Characterization of Zn-stimulated process of uptake

We investigated whether the Zn stimulatory effect involves modification of the membrane potential or the activation of voltage-gated Ca pathways (Fig. 6). As expected, neither 10 μM nifedipine nor verapamil modified the control accumulation values of Ca measured under standard external Na conditions (Na-crossed columns). Cells preincubated for 15-min in a Na^+-free (excess of K^+) nitrate medium, which should collapse the membrane potential, did not modify basal Ca uptake levels (compare both Ctrl Na and K columns), suggesting no activation of any voltage-dependent Ca transport process. Accordingly, nifedipine did not modify Ca uptake measured under K conditions, although verapamil led to a small but significant 17% inhibition. Regardless of the Na or the K medium, stimulation by Zn was not affected by nifedipine. However, verapamil led to a 30% lower stimulatory effect in the Na medium and completely eliminated it in the K medium.

Mg^{2+}, Ba^{2+}, $Gd^{3+}$and La^{3+} are often used to inhibit cationic transport pathways including voltage- or store-operated Ca^{2+} channels. Among these metals, only 1 mM Gd (Ctrl-black column) resulted in a 25% decrease in the basal (Ctrl-open column) accumulation of Ca (Fig. 7). 13% lower uptake values were obtained in the presence of 1 mM of either Mg (Ctrl-grey column), Ba (Ctrl-dashed column) and La (Ctrl-crossed column), but differences were not significant. However, Mg, Ba, Gd and La all three significantly decreased Zn-stimulated Ca uptake (Zn-columns): Mg and Ba lowered by half the stimulatory effect of Zn, Gd completely eliminated it, and La even led to a 37% decrease in uptake levels compared to control data measured in the absence of Zn.

The possible involvement of $P2X_4$ purinergic receptor channels in Zn-induced stimulation of Ca and Cd uptake in HIEC cells was tested [29–32]. RT-PCR analysis revealed very low levels of $P2X_4$ mRNA in post-confluent 10-day-old HIEC

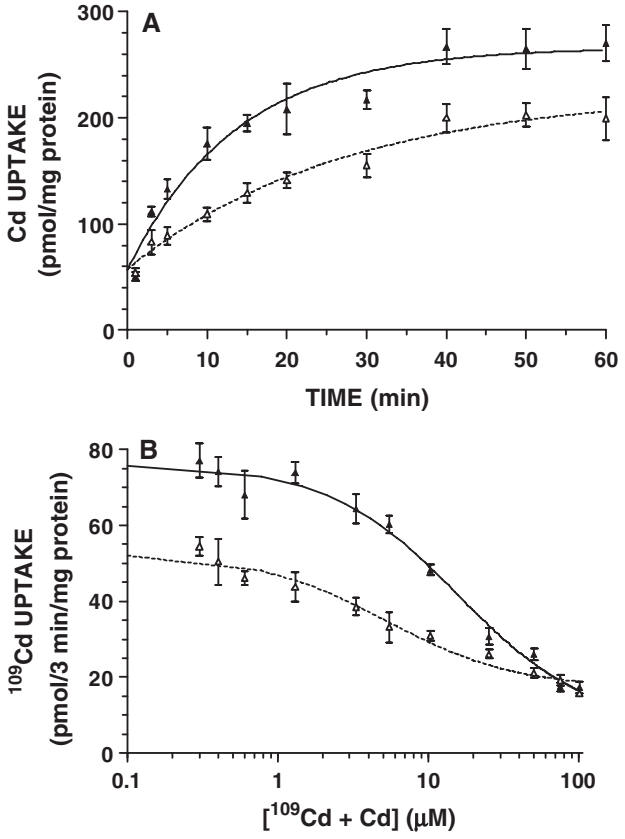

Fig. 5. (A) Time course of 0.3 μM Cd accumulation in 10-day-old HIEC cell monolayers in the absence (open triangles) or presence (filled triangles) of 100 μM Zn. Points shown are means±S.D. evaluated on 4 determinations of the same subculture. Lines shown are the best-fit curves for the data points as obtained according to the first-order rate Eq. (1) with uptake parameter values listed in Table 1. (B) Determination of kinetic parameters for ^{109}Cd uptake in HIEC cells in the absence (open triangles) or presence (filled triangles) of 100 μM Zn. Initial uptake values were estimated at 3 min using a ^{109}Cd concentration of 0.3 μM and unlabeled Cd concentrations ranging from 0 to 100 μM. Values shown are means±S.D. evaluated on 4 determinations of the same subculture. Lines shown are the best-fit curves for the data points as obtained according to Eq. (3). The kinetic parameter values are listed in Table 2.

cell monolayers as well as in undifferentiated proliferative TC7 cells. In contrast, 8- and 6-fold higher $P2X_4$ mRNA levels were detected in well-differentiated 21-day-old TC7 cells and 15-day-old A549 cells, respectively (Fig. 8). Because Zn-stimulated Ca and Cd uptakes were observed in the HIEC cells exclusively, it is unlikely that $P2X_4$ would be responsible for the stimulatory effect of Zn. Accordingly, neither 50 μM ATP,

Table 1
Parameter values describing the time course of 0.3 μM Cd uptake over a 60-min exposure in the absence or presence of Zn

	U_0 (pmol/mg protein)	U_{max} (pmol/mg protein)	$t_{½}$ (min)
Ctrl	57.8±7.4	167±15	20.3±5.1
Zn	56.8±15.1	210±16	9.9±2.2

Note. Ten-day-old HIEC cells were exposed to 0.3 μM ^{109}Cd in a Ca-free nitrate transport medium in the absence (Ctrl) or presence of 100 μM Zn. The meaning of the parameters U_0, U_{max} and $t_{½}$ is given in the text. The values shown are the best-fit parameters±SER values corresponding to Eq. (1).

Table 2
Kinetic parameter values of the initial 3-min uptake of Cd in the absence or presence of Zn

	V_{max} (pmol/3 min/mg protein)	K_m (μM)	k_D (pmol/3 min/mg protein/μM)
Ctrl	618±176	5.2±1.5	57.0±6.0
Zn	3617±841	15.7±3.2	23.7±11.9

Note. Ten-day-old HIEC cells were exposed to 0.3 μM ^{109}Cd in a Ca-free nitrate transport medium, in the presence of unlabeled Cd concentrations ranging from 0 to 100 μM, in the absence (Ctrl) or presence of 100 μM Zn. The parameters V_{max} and K_m have their usual meaning, whereas k_D represents all non-specific contributions to uptake. The values shown are the best-fit parameters±SER values corresponding to Eq. (3).

expected to increase Ca uptake, nor 30 μM suramin, a P2X antagonist, modified the 3-min accumulation of Ca in the HIEC cells (Fig. 9).

Another mechanism that could be responsible for the observed stimulation of Ca and Cd uptake by Zn may involve a Zn-sensing receptor (ZnR) that trigger the release of thapsigargin-sensitive Ca pool [33]. As expected, inhibition of the SERCA pumps with 5 μM thapsigargin led to Ca rise from intracellular pools and the subsequent activation of the SOCs (Fig. 10A, filled circles). Significant Ca influx from extracellular medium was also measured in control cells (open circles), but Ca influx was twice as high in cells pretreated with thapsigargin. Zn alone failed to mimic the effect of thapsigargin on intracellular Ca stores (data not shown) but co-incubation with Zn and Ca led to a 3-fold increase in intracellular Ca whether or not the cells were pretreated with 30 μM SFK-96365 (Fig. 10B). Similar results were obtained for the 3-min

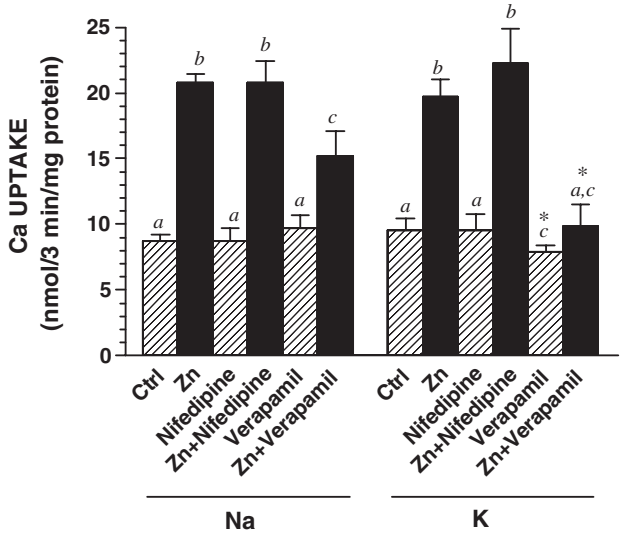

Fig. 6. Short-term (3 min) accumulation of 0.5 mM Ca in confluent 10-day-old HIEC cell monolayers in the absence (Ctrl) or presence of 100 μM Zn, 10 μM nifedipine or 10 μM verapamil, added alone or in various combinations to the nitrate medium. Experiments were conducted in a standard (141 mM Na^+) or in a Na^+-free (147 mM K^+) uptake medium in cells preincubated for 15 min in the respective medium. Values shown are means±S.D. evaluated on 5 determinations of the same subculture. Columns labeled with different letters are significantly different ($P \leq 0.05$). *Significant differences ($P \leq 0.05$) compared to the corresponding Na^+ condition.

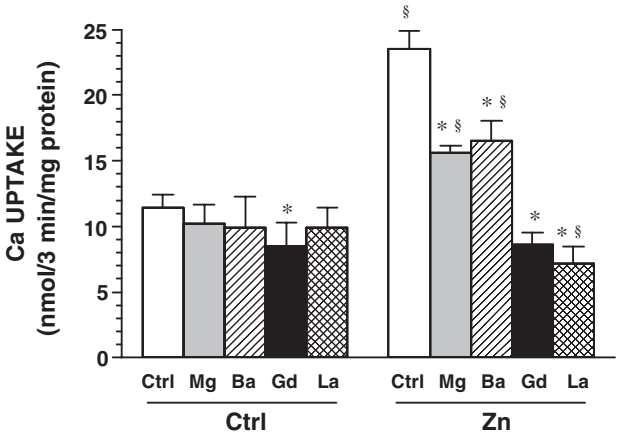

Fig. 7. Short-term (3 min) accumulation of 0.5 mM Ca in 10-day-old HIEC cells in the absence (Ctrl) or presence of 100 μM Zn (Zn) alone or in the presence of 1 mM of either Mg, Ba, Gd or La. Values shown are means ± S.D. evaluated on 4 determinations of the same subculture. *Significant differences ($P \leq 0.05$) compared with the value measured in the absence of Mg, Ba, Gd or La for each cell treatment. §Significant differences ($P \leq 0.05$) compared with similar uptake conditions on control cells (no co-exposure to Zn).

accumulation of 0.5 mM Ca: a 6-fold increase in uptake levels were measured following cells preincubation for 5 min with only 0.5 μM thapsigargin (grey column), and similar levels of stimulation were obtained with 100 μM Zn (black column). The inhibitory effect of SKF-96365 remains doubtful since co-incubation with Zn led to 23% decrease in Zn-induced stimulation, while preincubation with 30 μM SKF-96365 failed to have any significant effect. Also, Cd uptake was found insensitive to 2 μM U7312, whereas this PLC inhibitor lowered by 28% the stimulatory effect of Zn on Ca uptake (Fig. 12).

4. Discussion

Despite the fact that intestinal crypt cells, in addition to villus cells, are also the first target cells following metal ingestion, Cd transport and toxicity in these stem cells remain poorly studied. In recent studies, we have shown that Cd is significantly accumulated in human HIEC cells; uptake time course data over a 60-min exposure to 0.3 μM Cd in a defined chloride medium at pH 7.4 revealed a 3-fold higher equilibrium uptake value compared to the differentiated TC7 clone of the Caco-2 cells [11,19]. A specific transport system of similar affinity but of much higher capacity (20-fold higher) was also characterized in the HIEC compared to the TC7 cells. Contrary to what has been observed for the differentiated TC7 cells, a small but significant component of Cd uptake in the HIEC was inhibited by Ca as well as by La. In both in vitro models, Zn inhibited Cd uptake under standard exposure conditions using a Ca-containing medium. All together, these results suggest that the cellular accumulation of Cd in HIEC cells may in part be related to the transport processes responsible for Ca or Zn. However, they also showed different transport properties for Cd uptake in crypt and differentiated intestinal cells. This conclusion was further strengthened by the demonstration that NRAMP2 is involved in the uptake of Cd^{2+} in TC7 but not HIEC cells [12,19].

We now show that Zn may stimulate either Ca or Cd uptake, with reciprocal inhibition between Ca and Cd (Fig. 1) in HIEC but not TC7 cells (Fig. 2). Zn-stimulated Ca uptake was systematically observed, whereas 66% of the Cd uptake measurements were stimulated. For the first time, we also show that Zn modifies the kinetic parameters of Cd uptake (Fig. 5A). The increase in both the V_{max} and K_m values suggests activation of different transport processes, whereas the lower k_D value estimated for the non specific contribution remains to be clarified (Fig. 5B). The maximal stimulatory effect was always observed under nitrate exposure conditions maximizing the presence of the free Cd^{2+} cation. Therefore, Cd–Ca interaction likely involves extracellular Cd^{2+} and Ca^{2+} cation species, which could compete for a ionic channel.

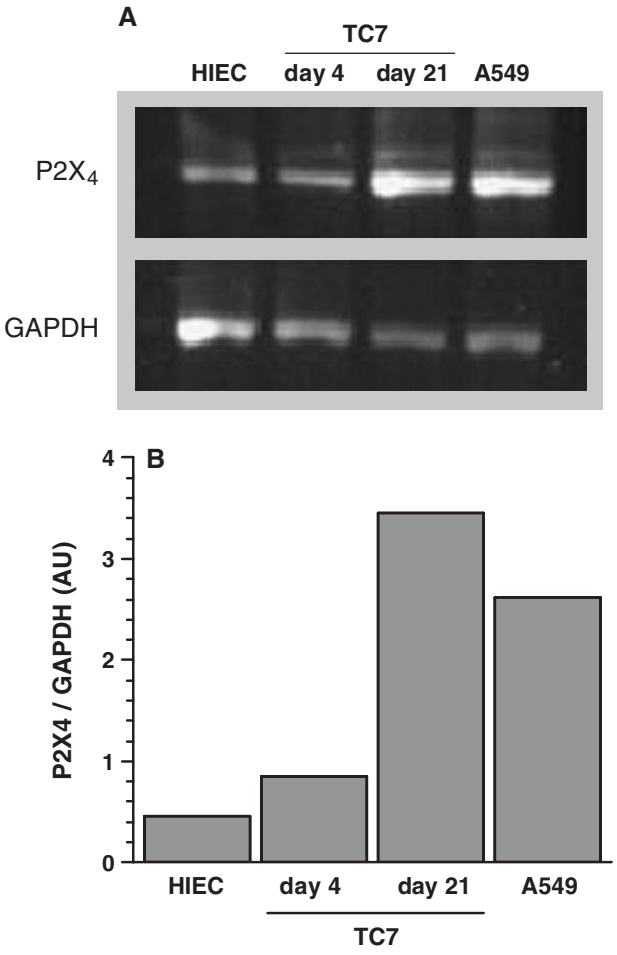

Fig. 8. (A) Representative RT-PCR amplification of $P2X_4$ and GAPDH mRNAs of 10-day-old HIEC cells, 4-day-old and 21-day-old TC7 cells, as well as 15-day-old A549 cell monolayers. Amplified products correspond to fragments 336–931 and 123–1066 of the $P2X_4$ and GAPDH cDNA, respectively. RT-PCR products were resolved by agarose gel electrophoresis as described in Materials and methods. (B) Image analysis of the amplified fragments allowed the $P2X_4$ mRNA expression levels to be normalized to the expression of the internal control GAPDH.

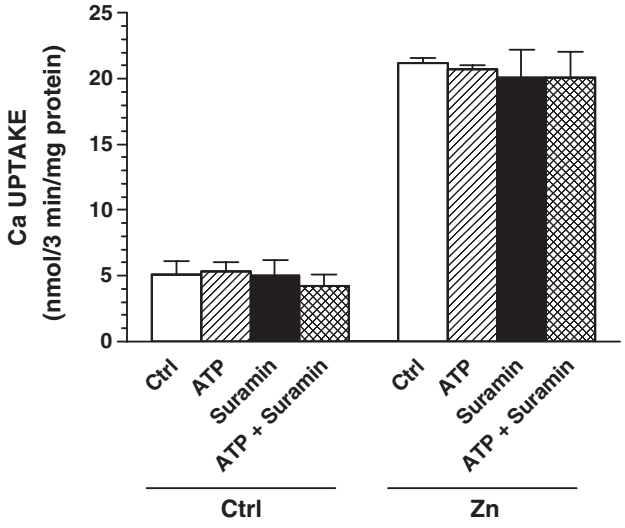

Fig. 9. Short-term (3 min) accumulation of 0.5 mM Ca in confluent 10-day-old HIEC cell monolayers in the absence (Ctrl) or presence of 100 μM Zn (Zn) alone or in the presence of 50 μM ATP or 30 μM suramin added alone or in combination. Values shown are means ± S.D. evaluated on 5 determinations of the same subculture.

This rather unexpected stimulation of Cd uptake by Zn has already been reported in rat red blood cells [40]. In these studies, however, Cd uptake measurements were conducted in a phosphate-buffered saline (PBS) which usually contains Ca (~1 mM). More recently, other investigators have reported Zn-stimulated increases in intracellular Ca in IB3-1 human airway epithelial cells [32], in primary cultures of rat hepatocytes [41], in Madin-Darby canine kidney (MDCK) cells [42], and in human intestinal HT-29 cells [33]. In accordance with our own results, these studies also revealed the involvement of concentration-dependent processes, with half-maximal effect ranging from 20 to 80 μM, indicating specific mechanisms of activation (Fig. 3). Moderate levels of Zn (10–50 μM) induced sustained increases in Ca influx in human airway cells IB3-1, whereas higher concentrations (200 μM) elicited transient rises in intracellular Ca followed by slower decreases, suggesting an inactivation mechanism [32]. In the HIEC cells, Zn at high concentration (1 mM) was much less efficient in stimulating the 3-min uptake of Cd as well as Ca (Fig. 4). More importantly, Zn-induced stimulation decreased with cell pretreatment with Zn in a concentration-dependent manner: the inward Zn gradient, rather than intracellular Zn, is responsible for the stimulatory effect (Fig. 4). In the hepatocytes and the HT-29 cells, the rise in cytosolic Ca was related to release from intracellular pools [33,41]. In contrast, influx of extracellular Ca was responsible for the increase in cellular Ca in the MDCK and the IB3-1 cells [32,42]. Basically, two main mechanisms have been proposed: Zn action through P2 receptors or through Zn-sensitive receptor (ZnR).

The purinoceptor superfamily P2 receptors recognize extracellular ATP, ADP, UTP and UDP. P2X receptors (P2XRs) are non-selective cation channels that allow influx of extracellular Ca [28], whereas P2Y receptors (P2YRs) are coupled to G protein activating PLC which in turn triggers the production of IP_3 leading to Ca mobilization from ER stores [37,43]. Among P2XRs, $P2X_4$ has been shown to be regulated by metal ions including Zn^{2+} and Cu^{2+}: Zn^{2+} favors ATP-stimulated $P2X_4$ activation, whereas Cu^{2+} inhibits it [31,32,44]. Because of its rapid inactivation, $P2X_3$, which is also sensitive to Zn, is generally believed not to be responsible for the observed sustained increase in Ca^{2+} influx [32]. Interestingly, Cd^{2+} has also been shown to mimic Zn's effect on Ca influx, which suggests no or very low Cd permeability through the activated mechanisms of transport [31]. In contrast, our data demonstrating reciprocal inhibition between Cd and Ca clearly show significant Cd permeability. Our results also reveal a higher stimulatory effect of Zn on Ca uptake compared to Cd, but the Ca concentration used in our studies was much higher (5 mM vs. 0.3 μM). As observed by others for $P2X_4$ activation [32], we found the stimulatory effect of Zn on Ca and Cd uptake in HIEC cells to decrease with acidic extracellular pH (data not shown). Also, Zn as well as Cu modulations of ATP-stimulated $P2X_4$ have been shown to be voltage-independent [31]. Changing Na

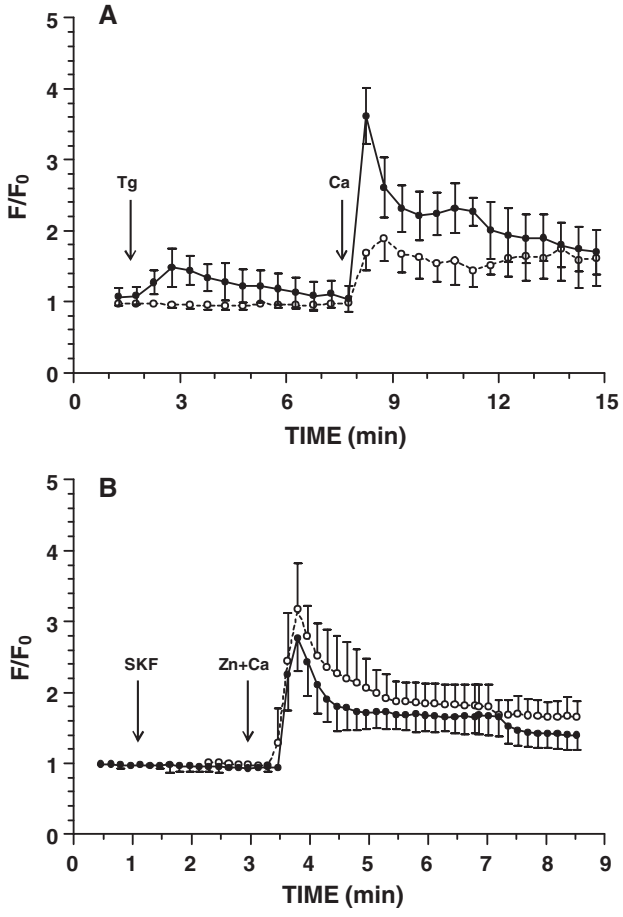

Fig. 10. Fluorescent change of Fluo-3/AM-loaded 5-day-old (60% confluent) HIEC cells. (A) thapsigargin (5 μM) was added (filled circles) or not (open circles) in the nitrate medium prior Ca addition (0.5 mM). (B) SKF-96365 (30 μM) was added (filled circles) or not (open circles) in the incubation medium prior Zn (100 μM) + Ca (0.5 mM) addition as mixture. Values shown are means fluorescence levels relative to control ± S.D. evaluated on 13 to 17 determinations of the same subculture.

for K, which is expected to collapse the transmembrane potential, did not affect either the basal or Zn-stimulated Ca uptake in the HIEC cells (Fig. 6). Therefore: (i) voltage-dependent Ca channels are unlikely to be expressed in these cells; and (ii) the stimulatory effect of Zn is not expected to involve activation of any voltage-gated channels. These conclusions are further supported by the lack of inhibition by nifedipine, even under exposure conditions with an excess of K^+. However, a clear inhibition of Zn-induced increase in Ca uptake was observed with verapamil. This specific effect of verapamil remains to be clarified, but nifedipine belongs to the dihydropyridin family of high selective L-type Ca channel blockers, whereas verapamil (a phenylalkylamin) is much less specific to Ca channels. Clearly, extracellular K does not potentiate Zn-induced stimulation of Ca uptake in HIEC cells. One important finding of our studies is the presence of Zn-induced stimulation of Ca uptake in the absence of extracellular ATP with no additional effect with co-incubation with ATP and Zn (Fig. 9). Suramin, a P2XRs antagonist, failed to block the effect of Zn. Although Zn-induced stimulation of Ca and Cd uptake was observed in HIEC cells but not in mature TC7 cells or in alveolar cells A549 (Fig. 2), 6- to 8-fold lower levels of $P2X_4$ mRNA were detected in HIEC cells (Fig. 8). Although Zn-stimulated Ca and Cd uptake in HIEC cells shares a number of features with the $P2X_4$ receptor channel, our results do not support Zn-modulated activation of $P2X_4$.

As for P2YRs, a metabotropic ZnR has been suggested to be responsible for Zn-induced release of Ca from ER stores through IP_3 transduction pathways [33,41]. This discharge of thapsigargin-sensitive intracellular pools may stimulate the influx of extracellular Ca through SOCs also called calcium-release-activated channel (CRAC). This capacitative Ca entry has been observed in the HIEC (Figs. 10A and 11). However, Zn alone failed to mimic the effect of thapsigargin on ER Ca stores, whereas co-incubation with Zn and Ca led to huge increases in Fluo-3 fluorescence (and uptake) levels without inhibition by SKF-96365 (Fig. 10B and 11). Only part (28%) of the Zn-stimulated Ca, but not Cd influx, was inhibited by U7312 (Fig. 12). Therefore, it is unlikely that Zn-induced stimulation of Ca and Cd uptake is mainly related to SOCs activation in response to Ca release from thapsigargin-sensitive stores.

Trivalent cations Gd^{3+} and La^{3+} are commonly used as blockers of non-selective cation channels [45,46], including Ca channels [47,48], while the divalent ion Ba^{2+} is a less potent inhibitor but often permeates Ca channels [49,50]. All of these metals showed a strong inhibitory effect on the Zn-stimulated uptake of Ca (Fig. 7), but Gd^{3+} and La^{3+} were more efficient compared to Ba^{2+}. La^{3+} was also shown to eliminate the Zn-stimulated rise in cytosolic [Ca] in MDCK cells [42]. The epithelial Ca channel CaT1 (also called TRPV6) is a member of the TRPV family of voltage-insensitive channels structurally related to the transient receptor potential (TRP) family of Ca

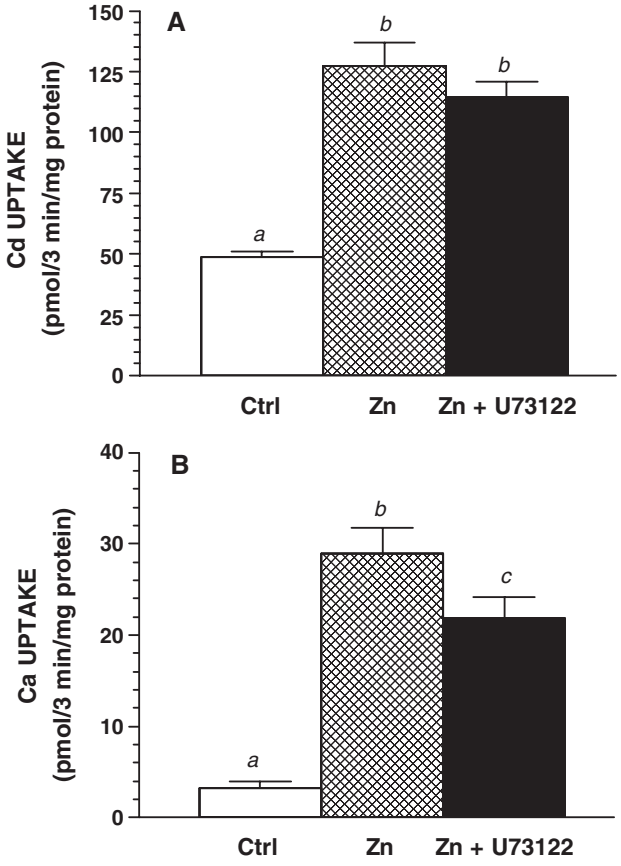

Fig. 12. Short-term (3 min) uptake of 0.3 μM Cd (A) or 0.5 mM Ca (B) in 10-day-old HIEC cells measured in the absence (Ctrl) or presence of 100 μM Zn alone or in combination with 2 μM U73122. Values shown are means ± S.D. evaluated on 5 determinations of the same subculture. Columns labeled with different letters are significantly different ($P \leq 0.05$).

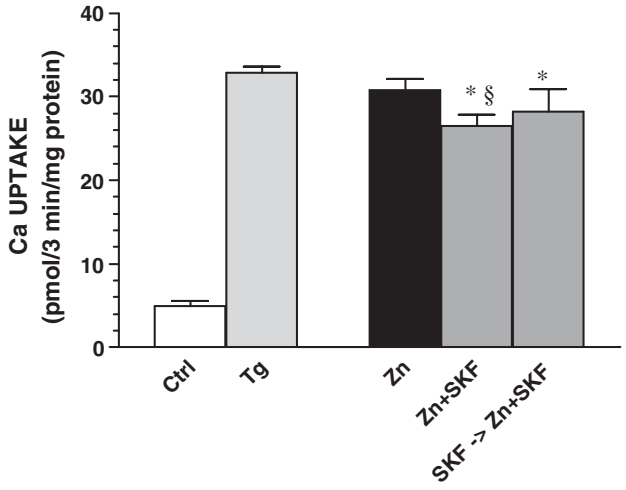

Fig. 11. Short-term (3 min) accumulation of 0.5 mM Ca in 10-day-old confluent HIEC cells in the absence (Ctrl) or the presence of 100 μM Zn alone or in combination with 30 μM SKF. Uptake experiments were also conducted on cells pretreated with 0.5 μM thapsigargin (Tg) for 5 min prior exposure to Ca or on cells pretreated with 30 μM SKF-96365 for 2 min prior co-exposure to Zn. Values shown are means ± S.D. evaluated on 5 determinations of the same subculture. *Significant differences ($P \leq 0.05$) compared with the value measured in the presence of thapsigargin. §Significant differences ($P \leq 0.05$) compared with uptake values measured in the presence of Zn alone.

channels [51]. Ca transport through CaT1 is highly inhibited by Gd^{3+} and La^{3+} (up to 85%) and to a much lesser extent (40%) by Ba^{2+} [42,45]. As already discussed in previous studies, we did not succeed in detecting significant CaT1 mRNA in HIEC cells [19], but our present results clearly show a Gd^{3+}- and La^{3+}-inhibitible Zn-stimulated mechanism of Ca uptake in HIEC cells. Because Zn was shown not to significantly modify Ca current in oocytes injected with CaT1 [52], the involvement of this epithelial Ca channel in the observed phenomenon in HIEC cells is unlikely. Also, because of its much stronger preference for Zn^{2+} over Ca^{2+} cation, the involvement of TRPM7 is unlikely [50].

5. Conclusion

In this study, we have further characterized Cd uptake in intestinal crypt HIEC cells. Our data provide evidence of reciprocal Ca and Cd inhibition for Zn-stimulated processes of uptake. These transport pathways are unlikely to involve voltage-gated channels but are inhibited by divalent metals and to a much higher extent by trivalent metals. Although Zn may activate the purinergic $P2X_4$ subtype of the P2X receptor channel, our results do not support the involvement of these channels in Zn-stimulated Ca and Cd uptake in HIEC cells. Also, Zn is unlikely to trigger the activation of SOCs in response to Ca release from thapsigargin-sensitive intracellular pools. Cd–Ca–Zn interactions for accumulation in intestinal crypt cells clearly deserve to be further investigated, especially since oral exposure to toxic metals generally involves metal mixtures. The present study demonstrates that, contrary to what is observed for differentiated enterocytes, Zn does not necessarily protect against the cellular accumulation of Cd, but instead may favor uptake processes.

Acknowledgements

The authors thank Marc Mantha and Dominique Labelle for their technical assistance with fluorescence studies and experiments testing the effects of thapsigargine, SKF and U7312. This work was supported by the Natural Sciences and Engineering Research Council of Canada, NSERC (Discovery grant, CJ, RGPIN-203202).

References

[1] F. Pinot, S.E. Kreps, M. Bachelet, P. Hainaut, M. Bakonyi, B.S. Polla, Cadmium in the environment: sources, mechanisms of biotoxicity, and biomarkers, Rev. Environ. Health 15 (2000) 299–323.
[2] D. Beyersmann, S. Hechtenberg, Cadmium, gene regulation, and cellular signalling in mammalian cells, Toxicol. Appl. Pharmacol. 144 (1997) 247–261.
[3] C. Jumarie, P.G.C. Campbell, M. Houde, F. Denizeau, Evidence for an intracellular barrier to cadmium transport through Caco-2 cell monolayers, J. Cell. Physiol. 180 (1999) 285–297.
[4] D.L. Hamilton, M.W. Smith, Inhibition of intestinal calcium uptake by cadmium and the effect of a low calcium diet on cadmium retention, Environ. Res. 15 (1978) 175–184.
[5] M. Ando, S. Matsui, Effect of cadmium on vitamin D-non-stimulated intestinal calcium absorption in rats, Toxicology 45 (1987) 1–11.
[6] P.M. Verbost, G. Flik, R.A.C. Lock, S.E. Wendelaar Bonga, Cadmium inhibits plasma membrane calcium transport, J. Membr. Biol. 102 (1988) 97–104.
[7] E.C. Foulkes, Interactions between metals in rat jejunum: implications on the nature of cadmium uptake, Toxicology 37 (1985) 117–125.
[8] D.E. Jaeger, Absorption interactions of zinc and cadmium in the isolated perfused rat intestine, J. Trace Elem. Electrolytes Health Dis. 4 (1990) 101–105.
[9] F. Tacnet, D.W. Watkins, P. Ripoche, Studies of zinc transport into brush-border membrane vesicles isolated from pig small intestine, Biochim. Biophys. Acta 1024 (1990) 323–330.
[10] J.P. Groten, E.J. Sinkeldam, T. Muys, J.B. Luten, P.J. van Bladeren, Interaction of dietary Ca, P, Mg, Mn, Cu, Fe, Zn and Se with the accumulation and oral toxicity of cadmium in rats, Food Chem. Toxicol. 29 (1991) 249–258.
[11] C. Jumarie, P.G.C. Campbell, A. Berteloot, M. Houde, F. Denizeau, Caco-2 cell line used as an in vitro model to study cadmium accumulation in intestinal epithelial cells, J. Membr. Biol. 158 (1997) 31–48.
[12] F. Elisma, C. Jumarie, Evidence for cadmium uptake through Nramp2: metal speciation studies with Caco-2 cells, Biochem. Biophys. Res. Commun. 285 (2001) 662–668.
[13] J. Tallkvist, C.L. Bowlus, B. Lönnerdal, DMT1 gene expression and cadmium absorption in human absorptive enterocytes, Toxicol. Lett. 122 (2001) 171–177.
[14] D.I. Bannon, R. Abounader, P.S.J. Lees, J.P. Bressler, Effect of DMT1 knockdown on iron, cadmium, and lead uptake in Caco-2 cells, Am. J. Physiol. 284 (2003) C44–C50.
[15] C. Jumarie, C. Fortin, M. Houde, P.G.C. Campbell, F. Denizeau, Cadmium uptake by Caco-2 cells: effects of Cd complexation by chloride, glutathione, and phytochelatins, Toxico. Appl. Pharmacol. 170 (2001) 29–38.
[16] C.J. Phillpotts, The autoradiographic localisation of retained orally administered cadmium tracer within Paneth cells of rat duodenum, Toxicology 33 (1984) 59–66.
[17] D. Hulinska, M. Vojtisek, D. Bittnerova, M. Cikrt, V. Hulinsky, Effect of cadmium on the rat intestine, Acta Morphol. Hung. 36 (1988) 121–132.
[18] M.R. Hughes, J.E. Smits, J.E. Elliott, D.C. Bennett, Morphological and pathological effects of cadmium ingestion on Pekin ducks exposed to saline, J. Toxicol. Environ. Health 61 (2000) 591–608.
[19] P.M. Bergeron, C. Jumarie, Characterization of Cd uptake in the human intestinal crypt cells HIEC in relation to inorganic metal speciation, Toxicology 219 (2006) 156–166.
[20] N. Perreault, J.F. Beaulieu, Use of the dissociating enzyme thermolysin to generate viable human normal intestinal epithelial cell cultures, Exp. Cell Res. 224 (1996) 354–364.
[21] R. Gauthier, C. Harnois, J.F. Drolet, J.C. Reed, A. Vezina, P.H. Vachon, Human intestinal epithelial cell survival: differentiation state-specific control mechanisms, Am. J. Physiol. 280 (2001) C1540–C1554.
[22] M.J. Boucher, D. Jean, A. Vezina, N. Rivard, Dual role of MEK/ERK signaling in senescence and transformation of intestinal epithelial cells, Am. J. Physiol. 286 (2004) G736–G746.
[23] N. Desloges, N. Basora, N. Perreault, Y. Bouatrouss, D. Sheppard, J.F. Beaulieu, Regulated expression of the integrin $\alpha 9\beta 1$ in the epithelium of the developing human gut and in intestinal cell lines: relation with cell proliferation, J. Cell. Biochem. 71 (1998) 536–545.
[24] F. Escaffit, N. Perreault, D. Jean, C. Francoeur, E. Herring, C. Rancourt, N. Rivard, P.H. Vachon, F. Pare, M.P. Boucher, J. Auclair, J.F. Beaulieu, Repressed E-cadherin expression in the lower crypt of human small intestine: a cell marker of functional relevance, Exp. Cell Res. 302 (2005) 206–220.
[25] C. Deschenes, L. Alvarez, M.E. Lizotte, A. Vezina, N. Rivard, The nucleocytoplasmic shuttling of E2F4 is involved in the regulation of human intestinal epithelial cell proliferation and differentiation, J. Cell Physiol. 199 (2004) 262–273.
[26] C. Harnois, M.J. Demers, V. Bouchard, K. Vallee, D. Gagne, N. Fujita, T. Tsuruo, A. Vezina, J.F. Beaulieu, A. Cote, P.H. Vachon, Human intestinal epithelial crypt cell survival and death: complex modulations of Bcl-2

homologs by Fak, PI3-K/Akt-1, MEK/Erk, and p38 signaling pathways, J. Cell. Physiol. 198 (2004) 209–222.
[27] F.M. Ruemmele, J.F. Beaulieu, J. O'Connell, M.W. Bennett, E.G. Seidman, M.J. Lentze, The susceptibility to Fas-induced apoptosis in normal enterocytes is regulated on the level of cIAP1 and 2, Biochem. Biophys. Res. Commun. 290 (2002) 1308–1314.
[28] R.A. North, Molecular physiology of P2X receptors, Physiol. Rev. 82 (2002) 1013–1067.
[29] F. Soto, M. Garcia-Guzman, J.M. Gomez-Hernandez, M. Hollman, C. Karshin, W. Stühmer, P2X4: an ATP-activated ionotropic receptor cloned from rat brain, Proc. Natl. Acad. Sci. U. S. A. 93 (1996) 3684–3688.
[30] K. Nakazawa, Y. Ohno, Effects of neuroamines and divalent cations on cloned and mutated ATP-gated channels, Eur. J. Pharmacol. 325 (1997) 101–108.
[31] C. Acuña-Castillo, B. Morales, J.P. Huidobro-Toro, Zinc and copper modulate differentially the P2X4 receptor, J. Neurochem. 74 (2000) 1529–1537.
[32] A. Zsembery, J.A. Fortenberry, L. Liang, Z. Bebok, T.A. Tucker, A.T. Boyce, G.M. Braunstein, E. Welty, P.D. Bell, E.J. Sorscher, J.P. Clancy, E.M. Schwiebert, Extracellular zinc and ATP restore chloride secretion across cystic fibrosis airway epithelia by triggering calcium entry, J. Biol. Chem. 279 (2004) 10720–10729.
[33] M. Hershfinkel, A. Moran, N. Grossman, I. Sekler, A zinc-sensing receptor triggers the release of intracellular Ca^{2+} and regulates ion transport, Proc. Nat. Acad. Sc. U. S. A. 98 (2001) 11749–11754.
[34] I. Chantret, A. Rodolosse, A. Barbat, E. Dussaulx, E. Brot-Laroche, A. Zweibaum, M. Rousset, Differential expression of sucrase-isomaltase in clones isolated from early and late passages of the cell line Caco-2: evidence for glucose-dependent negative regulation, J. Cell Sci. 107 (1994) 213–225.
[35] W.D. Schecher, D.C. McAvoy, MINEQL^{+}: A Chemical Equilibrium Program for Personal Computers, Environmental Research Software, Hallowell, ME (1994) Version 3.01.
[36] A.E. Martell, R.M. Smith, R.J. Motekaitis, NIST Critically Selected Stability Constants of Metal Complexes Database, United States Department of Commerce, Gaithersburg, MD (2001) Version 6.0.
[37] E.A. Barnard, G. Burnstock, T.E. Webb, G protein-coupled receptors for ATP and other nucleotides: a new receptor family, Trends Pharmacol. Sci. 15 (1994) 67–70.
[38] A. Bouron, X. Alrafai, S. Boisseau, M. DeWaard, A store-operated Ca^{2+} influx activated in response to the depletion of thapsigargin-sensitive Ca^{2+} stores is developmentally regulated in embryonic cortical neurons from mice, Dev. Brain Res. 159 (2005) 64–71.
[39] M.M. Bradford, A rapid and sensitive method for the quantitation of microgram quantities of protein utilizing the principle of protein-dye binding, Anal. Biochem. 72 (1976) 248–254.
[40] M. Garty, W.M. Bracken, C.D. Klaassen, Cadmium uptake by rat red blood cells, Toxicology 42 (1986) 111–119.
[41] T.J. McNulty, C.W. Taylor, Extracellular heavy-metal ions stimulate Ca^{2+} mobilization in hepatocytes, Biochem. J. 339 (1999) 555–561.
[42] C.R. Jan, S.N. Wu, C.J. Tseng, Zn^{2+} increases resting cytosolic Ca^{2+} levels and abolishes capacitative Ca^{2+} entry induced by ATP in MDCK cells, Naunyn-Schmiedeberg's Arch. Pharmacol. 360 (1999) 249–255.
[43] V. Ralevic, G. Burnstock, G, Receptors for purines and pyrimidines, Pharmacol. Rev. 50 (1998) 413–492.
[44] A. Zsembery, A.T. Boyces, L. Liang, J. Peti-Peterdi, P.D. Bell, E.M. Schwiebert, Sustained calcium entry through P2X nucleotide receptor channels in human airway epithelial cells, J. Biol. Chem. 278 (2003) 13398–13408.
[45] K. Manabe, M. Takano, A. Noma, Non-selective cation current of guinea-pig endocardial endothelial cells, J. Physiol. 487 (1995) 407–419.
[46] M. Suzuki, M. Murata, M. Ikeda, T. Miyoshi, M. Imai, Primary structure and functional expression of a novel non-selective cation channel, Biochem. Biophys. Res. Commun. 242 (1998) 191–196.
[47] B.N. Ling, W.C. O'Neill, Ca^{2+}-dependent and Ca^{2+}-permeable ion channels in aortic endothelial cells, Am. J. Physiol. 263 (1992) H1827–H1838.
[48] R. Vennekens, J. Prenen, J.G.J. Hoenderop, R.J.M. Bindels, G. Droogmans, B. Nilius, Pore properties and ionic block of the rabbit epithelial calcium channel expressed in HEK 293 cells, J. Physiol. 530 (2001) 183–191.
[49] J.G.J. Hoenderop, A.W.C.M. van der Kemp, A. Hartog, S.F.J. van de Graaf, C.H. van Os, G.M. Willems, R.J.M. Bindels, Molecular identification of the apical Ca^{2+} channel in 1,25-dihydroxyvitamin D3-responsive epithelia, J. Biol. Chem. 274 (1999) 8375–8378.
[50] M.K. Monteilh-Zoller, M.C. Hermosura, M.J.S. Nadler, A.M. Scharenberg, R. Penner, A. Fleig, TRPM7 provides an ion channel mechanism for cellular entry of trace metal ions, J. Gen. Physiol. 121 (2003) 49–60.
[51] X. Zhu, M. Jiang, M. Peyton, G. Boulay, R. Hurst, E. Stefani, L. Birnbaumer, TRP, a novel mammalian gene family essential for agonist-activated capacitative Ca^{2+} entry, Cell 85 (1996) 661–671.
[52] J.B. Peng, X.Z. Chen, U.V. Berger, P.M. Vassilev, H. Tsukaguchi, E.M. Brown, M.A. Hediger, Molecular cloning and characterization of a channel-like transporter mediating intestinal calcium absorption, J. Biol. Chem. 274 (1999) 22739–22746.